

Preparation of Dental Hard Tissue with Picosecond Laser Pulses

LÜKO WILLMS^a, ANDREA HERSCHEL^b, MARK H. NIEMZ^b, THOMAS PIOCH^c

^aPhysikalisch-Chemisches Institut, Germany

^bInstitut für Angewandte Physik, Germany

^cPoliklinik für Zahnerhaltungskunde, Universität Heidelberg, Germany

Correspondence to L. Willms, Physikalisch-Chemisches Institut (PCI), INF 253, D-69120 Heidelberg, Germany

Paper received 8 August 1995

Abstract. The aim of this study was to investigate the suitability of picosecond lasers for hard-tissue preparation. Using scanning electron microscopy (SEM) and histological studies, the quality of ablation was examined. There was no thermal or mechanical damage observed. The ablation rates of enamel, dentine and carious enamel and the temperature rise during tissue removal were measured. Using a fast silicon photodiode, the lifetime of the plasma was determined to be 11 ± 3 ns (Nd-YLF, $1.25 \text{ mJ pulse}^{-1}$, pulse duration 30 ps). In order to achieve a better understanding of the ablation process, plasma parameters such as electron density [$(5 \pm 3) \times 10^{17} \text{ cm}^{-3}$] and excitation temperature (4500 ± 2000 °K, Nd-YLF, $0.3 \text{ mJ pulse}^{-1}$) were obtained from emission spectra. By examining the line width of singly ionized calcium lines, a difference was found in the ablation of healthy or artificially demineralized enamel, thus allowing the selective removal of caries.

INTRODUCTION

Since lasers were invented in 1960, several attempts have been made to apply lasers to certain procedures in dentistry, especially in the therapy of caries. Caries develops when lack of oral hygiene encourages microorganisms to form lactic and acetic acid which dissolve hydroxyapatite in dental enamel and dentine. One aim of using lasers in dentistry is to achieve a more accurate and painless treatment of caries by replacing conventional drilling machines with lasers. Since pain is usually caused by vibration and heat due to friction, it can probably be reduced by using a contactless operating laser that is working in the 'cold' ablation range. Cw lasers and pulsed lasers with pulse durations in the microsecond range usually generate too much heat during the ablation process. This is due to the fact that in this time frame, heat diffusion plays a very important role in the interaction mechanism, which is a thermal interaction (1). The first lasers ever used in dentistry, the ruby laser (2, 3) and the CO₂ laser (4, 5), are representatives of this group. They show very strong thermal side-effects; the temperature in the

inner tooth increases by more than 10 °C, thereby injuring the pulp tissue irreversibly (6, 7).

Meanwhile, several experiments have been performed using alternative laser systems, such as the erbium-yttrium aluminium garnet (Er-YAG) laser (8-10) and Excimer lasers, especially the argon fluoride (ArF) laser (11, 12). The wavelength of the Er-YAG laser, at $2.94 \mu\text{m}$, matches a resonance frequency of vibrational oscillations of water molecules contained in teeth, thereby enhancing the absorption of Er-YAG radiation drastically. This absorption leads to explosive vaporization that breaks the hydroxyapatite structure. So far, only free-running Er-YAG lasers with pulse durations in the microsecond range have been investigated because of the difficulty in mode-locking this laser type whilst maintaining a sufficient energy output. The coincidence of thermal and mechanical ablation effects has led to the term 'thermomechanical' interaction (10). However, due to a higher water content in the striae of Retzius, microcracks, that are up to $300 \mu\text{m}$ deep, are induced by this type of interaction. These cracks may lead to new caries development (13).

The ArF laser, at a wavelength of 193 nm, operates with shorter pulse durations, typically of 15 ns, and therefore generates fewer heat-induced ruptures. However, the ablation rate, ie the ablated volume per pulse, is not sufficient for clinical application (14). This low effectiveness and the general risks of u.v. radiation are the major disadvantages concerning the use of ArF lasers in dentistry, although it may be of importance for other medical applications.

In this study, the ablation of dental substances by means of picosecond laser pulses is investigated. Previous results have been reported elsewhere (15, 16). By focusing a short laser pulse on a tooth surface, energy densities in the range of 10^{12} W cm⁻² are reached. Ionizing the tissue leads to microplasma formation with a specific electron density, electron excitation temperature and lifetime. Using pulse durations in the μ s and ns ranges, the expansion of the hot plasma primarily results in a shock wave ablating the surrounding tissue. When applying shorter pulses, not only the diffusion of heat, but also the expansion of the plasma during the incident laser pulse, can be neglected, therefore reducing the extent of potential side-effects.

Another advantage of such short pulse durations is the fact that the spectroscopic analysis of laser-induced plasma sparks enables a novel diagnostic technique for caries as shown in the present paper.

MATERIALS AND METHODS

Lasers

Two different picosecond laser systems were used to perform the experiments. Most of the results were carried out using a short pulse, high repetition rate neodymium-yttrium lithium fluoride (Nd-YLF) laser system which is described in detail by Niemz (15). It was designed as a two-stage oscillator/regenerative amplifier combination with an emission wavelength of 1053 nm. Pulse energies of up to 1.25 mJ at up to 1 kHz repetition rate could be used. Autocorrelation of pulses showed that pulse durations were around 30 ps.

A commercial neodymium-yttrium aluminium garnet (Nd-YAG) picosecond laser (Continuum PY 61C-20) with similar features as the Nd-YLF was also used for experiments. This laser was actively and passively mode-

locked in the same cavity, and laser pulses were dumped with a Pockels cell. Repetition rates of 20 Hz were thereby obtained, and pulse energies of 2.5 mJ at pulse durations of 40 ps were used.

Tooth preparation

The ablation tests were carried out on 50 freshly extracted human molars which had been stored in buffered saline. The teeth were kept wet during the tests. In order to achieve demineralization after laser treatment, the teeth were stored in lactic acid for 6 weeks. For the ablation process, teeth were fixed on a stage that could be positioned by computer-controlled stepping motors. Different sized cavities were produced by moving the teeth within the focus of the laser beam.

Enamel cavities were created in the cervical enamel (Nd-YLF, 160 000 pulses, 1 mJ pulse⁻¹); for dentine cavities, the laser beam was focused parallel to the dentine tubules (Nd-YLF, 30 000 pulses, 0.7 mJ pulse⁻¹) of three teeth after cutting the clinical crowns. For SEM evaluations, the specimens were coated with a gold layer of 30 nm.

For histological examination, two extracted wisdom teeth were used and cavities were generated in the cervical enamel immediately after extraction in order to avoid the drying of the tooth (Nd-YLF, 50 000 pulses, 0.75 mJ pulse⁻¹). For fixation, the teeth were stored in a buffered 10% formalin solution for 14 days. They were totally demineralized in EDTA (25%), embedded in methacrylate, and sections of 3 μ m thickness were cut with a microtome. Finally, they were stained by the method of Ladewig (17).

Ablation measurements

Ablation was examined in healthy enamel ($n=10$ teeth), carious enamel ($n=10$ teeth), and dentine ($n=15$ teeth). The laser beam was focused perpendicularly on to the specimens' surfaces, using a SiO₂ lens ($f=50$ mm). As a rule, the diameter of the produced cavity of a single laser shot is only about 20 μ m wide, which makes it difficult to determine the cavity depth exactly, even when using an electron microscope. Therefore, cavities were prepared by scanning the laser beam over the surface. The distance between the particular focal

spots was chosen to be $20\ \mu\text{m}$ to prevent the overlap of adjacent pulses. By using a pattern of 10×60 spots, the obtained lateral cavity size was $200\ \mu\text{m} \times 1200\ \mu\text{m}$. A constant number of laser pulses was applied to each spot.

By means of a diamond saw, the teeth were cut perpendicularly to the longest sides of the cavities into $0.2\ \text{mm}$ thick slices. The cavity depth was determined using a light microscope and an ocular micrometer. For each data point, results obtained from five measurements were averaged.

Temperature measurements

The temperature measurements were carried out on 15 extracted healthy teeth. The temperature rise was detected by a silicon resistance sensor built into the pulp chamber. The remaining volume of the pulp chamber was filled with water to guarantee thermal contact. Rectangular cavities were created on a surface of $0.5\ \text{mm} \times 0.5\ \text{mm}$ using the computer-controlled stage. The distance between adjacent pattern points was $20\ \mu\text{m}$, while the number of pulses per pattern point was varied. The laser energy used was $650\ \mu\text{J pulse}^{-1}$.

Spectroscopic analysis

While ablating enamel ($n=5$ teeth), the lifetime of the laser-induced plasma was measured with a fast silicon photodiode (FND 100) having a rise time of about $1\ \text{ns}$ and a spectral sensitivity ranging from $0.35\ \mu\text{m}$ to $1.1\ \mu\text{m}$, with a maximum around $0.9\ \mu\text{m}$. The signals were read out by a Tektronix DSA 602 digitizing signal analyser. Due to the high sensitivity of the photodiode within the range of the laser wavelength, an infra-red filter (BK7) was used to suppress the laser light that was reflected from the plasma and the surface. To be able to compare the temporal behaviour of the plasma luminescence with that of the laser pulse, both were measured separately using the same trigger signal from the laser Pockels cell.

Emission spectra of the plasma were recorded using two independent methods. While ablating enamel ($n=6$ teeth) with the Nd-YLF laser, plasma spectra were obtained in a scanning mode with a monochromator (Jobin Yvon HR640, $f=1\ \text{m}$) controlled by a stepping motor. The signal was detected with a

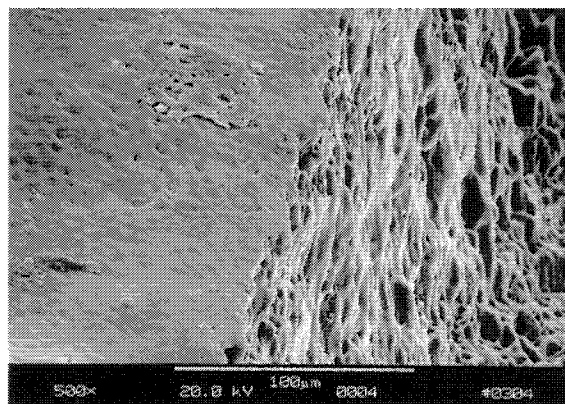


Fig. 1. Scanning electron microscopy of cavity edges after laser exposure (left: enamel surface, right: cavity wall).

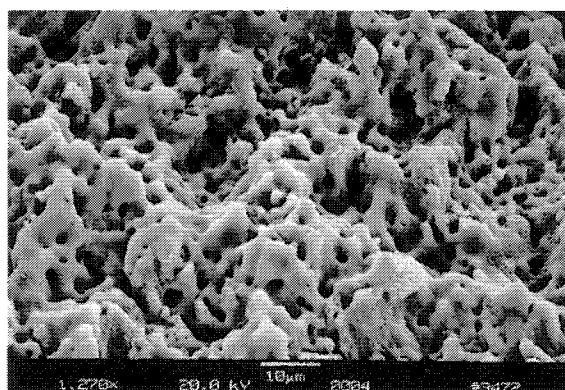


Fig. 2. Scanning electron microscopy of cavity bottom in enamel.

photomultiplier tube (Hamamatsu 1463 R) and a gated electronic system. All scans were recorded in 0.04-nm increments, each increment averaging 10 laser pulses. Spectra were also acquired in broadband mode using a SPEX 1877 $f=0.6\ \text{m}$ triple spectrometer and an intensified diode array (EG&G 1460). The data were recorded with an optical multichannel analyser (EG&G, OMA III System) while ablating healthy ($n=10$ teeth) and carious enamel ($n=10$ teeth). For each spectrum, over 70 pulse signals were averaged.

RESULTS

Cavity examination

The surfaces of the cavity walls are smooth and appear glasslike (Fig. 1). The roughness of the cavity bottom is about $10\ \mu\text{m}$ (Fig. 2). In dentine, the openings of dentine tubules are visible (Fig. 3) and fractures of the cavity edges

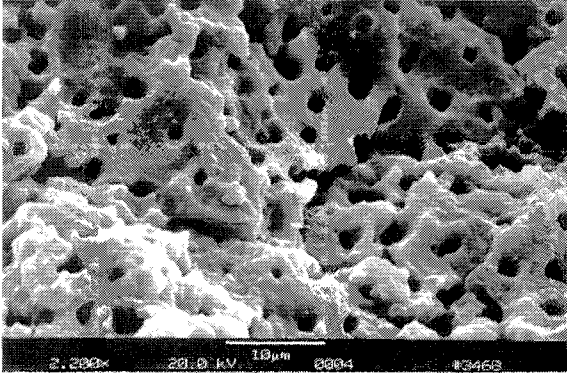


Fig. 3. Scanning electron microscopy of cavity bottom in dentine.

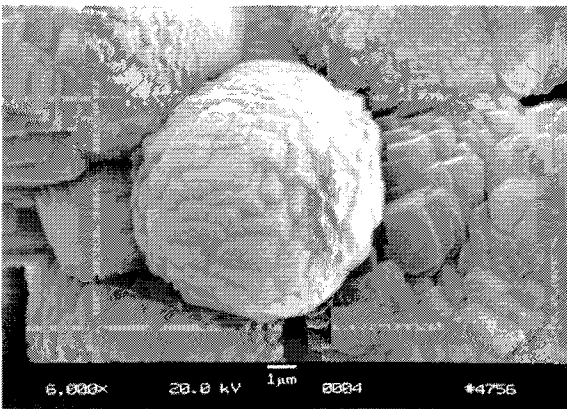


Fig. 4. Scanning electron microscopy of recrystallization structures on the cavity wall.

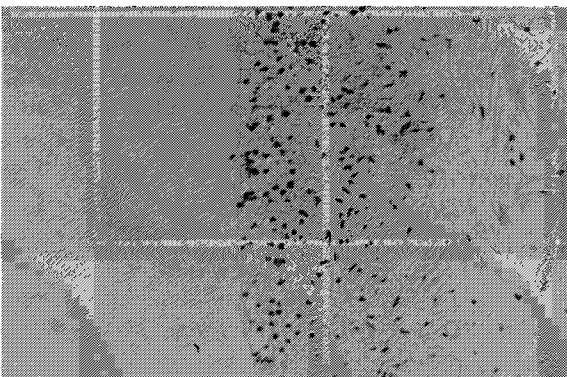


Fig. 5. Histological image of pulp (right) dentine (left) junction.

in dentine reach $30\ \mu\text{m}$. If the spatial distance of consecutive laser pulses is diminished, isolated structures with crystalline-like edges appear (Fig. 4). In histological images, the typical odontoblast layer is visible (Fig. 5). Pathological structures could not be identified.

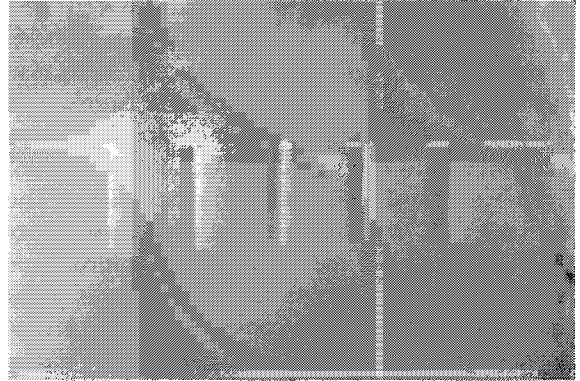


Fig. 6. Five cavities ($1.2\ \text{mm} \times 0.2\ \text{mm}$) in dentine obtained with increasing pulse energy from left to right ($400\ \mu\text{J}$, $575\ \mu\text{J}$, $625\ \mu\text{J}$, $725\ \mu\text{J}$, $850\ \mu\text{J}$).

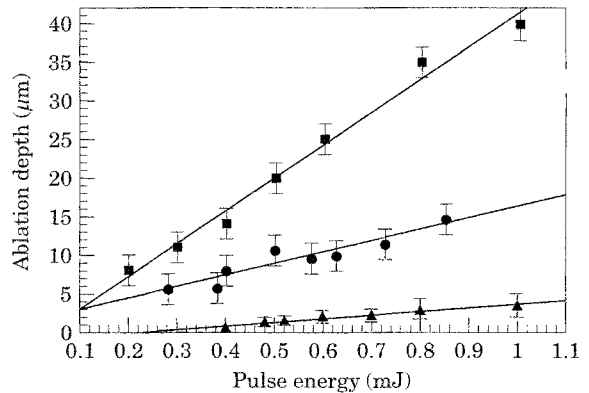


Fig. 7. Cavity depth per laser pulse as a function of the pulse energy for carious enamel (■), dentine (●), and healthy enamel (▲).

Ablation measurements

Figure 6 shows five dentine cavities obtained by different laser pulse energies. The cavity depth per laser pulse for different tooth substances as a function of the laser pulse energy is shown in Fig. 7. The resulting cavity depths depend linearly on the pulse energy within the entire measuring range. The fitted slopes are $5\ \mu\text{m}\ \text{mJ}^{-1}$ for enamel, $15\ \mu\text{m}\ \text{mJ}^{-1}$ for dentine and $43\ \mu\text{m}\ \text{mJ}^{-1}$ for carious enamel. Using a pulse energy of $1\ \text{mJ}$, the ablated volume per pulse is 10 times higher for dentine than for enamel. The highest ablation efficiency was observed in the case of carious enamel. At $1\ \text{mJ}$, it is about 10 times higher than that of healthy enamel.

Temperature measurements

The pulp temperature evolution for the application of 10 pulses per focal spot is shown in

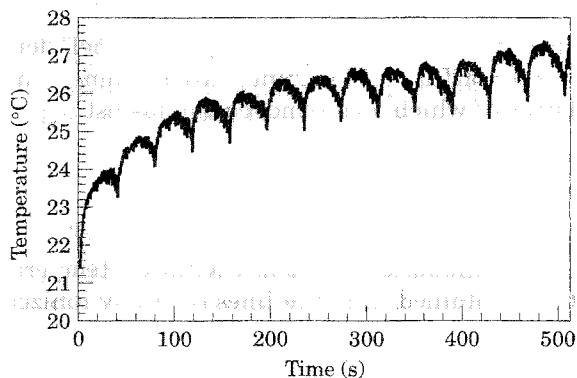


Fig. 8. Typical temperature development in the pulp vs time (10 pulses per focal spot, 130 Hz overall pulse repetition rate).

Fig. 8. Every 40 s, a temperature decrease appears as a result of re-setting the stage after the completion of the pattern. While the stage moved back to the start position, no laser pulse was applied to the tooth, and the heat diffused into the surrounding tissue. The distance between the temperature probe and the plasma was roughly 1 mm and decreased when, during the application of laser pulses, dental hard substances were ablated. The noise in the voltage signal (Fig. 8) is caused by electrical interferences of the Pockels cell of the laser and the stepping motors. The temperature curve shows a steep increase during the first 30 s, with an average temporal temperature gradient of about $5^{\circ}\text{C min}^{-1}$. With increasing time, this curve flattens so that after about 3 min, the average temperature increased almost linearly with a gradient of about $0.16^{\circ}\text{C min}^{-1}$. This qualitative temperature response was typical of all measurements.

The temperature increase was dependent on both the pulse repetition frequency of the laser and also on the frequency at which the laser focus was moved from one spot to the next. When a single pulse was applied per spot, the pulse repetition rate equalled the frequency of the stepping motor (≈ 20 Hz). However, when the number of pulses per spot was 5, 10 or 30, these consecutive pulses were delivered at the laser frequency of 400 Hz. In between the pulse trains, there was a gap of about 50 ms caused by the 20 Hz movement of the stepping motor. Even after 10 min of laser irradiation, the temperature increase for the patterns with one to five pulses per spot was below 3°C . The maximum temperature increase was 4°C with a pattern of 10 pulses per spot and 7°C with a pattern of 30 pulses per spot after 3 min of laser irradiation.

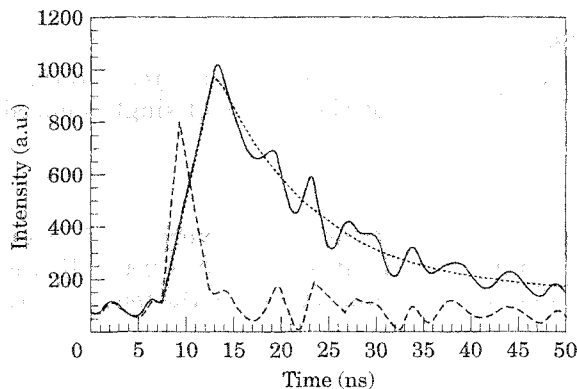


Fig. 9. Photodiode signal of plasma (—) and laser pulse (---). . . ., exponential fit, $t=11\pm 3$ ns.

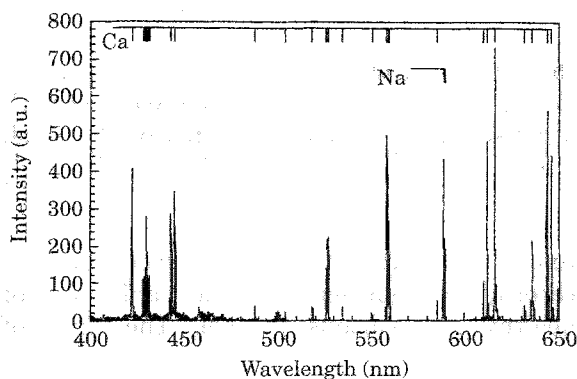


Fig. 10. Plasma emission spectrum while ablating enamel (Nd-YLF laser, $325\ \mu\text{J pulse}^{-1}$). Lines of neutral and singly ionized calcium, as well as the sodium-D-doublet, can be seen.

Spectroscopic analysis

In Fig. 9, a typical measurement of the plasma lifetime is shown. The relative intensity of the photodiode signal is plotted vs time. For comparison, the signal of the reflected laser pulse is also illustrated. The duration of the laser pulse is 30 ps but cannot be resolved due to the long rise time of the photodiode. A weaker second laser pulse is dumped from the cavity as well. The luminescence of the plasma is characterized by a fast initial rise time followed by slower exponential decay. The average duration ($1/e$ value) of the plasma emission was found to be $11(\pm 3)$ ns ($1.25\ \text{mJ pulse}^{-1}$). The dotted line shows an exponential fit. Noise in the signal is mainly due to the Pockels cell.

Figure 10 shows a spectrum of the plasma during the ablation of enamel with the Nd-YLF laser. The pulse duration was 30 ps, the pulse energy $325\ \mu\text{J}$. From this spectrum, lines of neutral and singly ionized calcium as

well as the D-doublet of sodium can be clearly identified (18).

In order to derive the plasma temperature, the intensities of eight lines of singly ionized calcium, at wavelengths ranging from 425 to 520 nm, were compared with eight lines measured at wavelengths of 610–650 nm. Using Boltzmann statistics, an average electron excitation temperature of $4500(\pm 2000)$ °K was calculated. The uncertainty in the temperature is mainly due to the variation in plasma temperature between single shots depending on the laser focus.

To obtain electron densities, the full width at half maximum (FWHM) of specific lines was measured and Stark broadening calculations were used (19, 20). Ablating enamel with the Nd-YLF laser with a pulse energy of 0.3 mJ, the plasma electron density was found to be $(5 \pm 3) \times 10^{17} \text{ cm}^{-3}$. For the Nd-YAG laser with a considerably higher pulse energy of 2.5 mJ, the calculations resulted in electron densities of $(6 \pm 2) \times 10^{18} \text{ cm}^{-3}$.

Examining the shape of the ionized calcium lines, a difference is visible between the recordings representing the ablation of healthy and carious enamel. The lines of demineralized enamel are broader by factors of 1.46 ± 0.2 at 393 nm and 1.54 ± 0.3 at 396 nm (FWHM, Nd-YAG) compared to those of healthy enamel, and the dips in the centre of the lines are deeper.

DISCUSSION

After the laser preparation of dentine, dentinal tubules were opened. In contrast, the application of conventional drilling instruments generates a smear layer that closes the tubules and thereby prevents the flow of liquid dentine. Thus, the application of conventional methods keeps the prepared surface relatively dry. As a clinical consequence of laser ablation, wet surfaces are present in dentine, where filling materials have to be applied.

Histological investigations should show whether laser-induced shock waves have a histologically visible effect on the pulp tissue or the region of the dentino-enamel junction. Such effects were not observed. However, in these experiments, the reaction of living pulp was not investigated and damage can therefore not be excluded. Therefore, the suitability of the in vivo application of the Nd-YLF laser in patients has yet to be confirmed.

The ablation measurements showed a difference in the ablation efficiency in enamel, dentine or artificially demineralized enamel, the latter of which was removed the fastest.

In the plasma spectra, strong lines of calcium and sodium were identified. On the other hand, no lines of phosphorus from this major component in human teeth could be seen.

The calculated electron excitation temperatures obtained from the lines of singly ionized calcium were all in the same range of 4500 °K, therefore verifying the assumption of a Boltzmann distribution. However, it is important to note that the reported temporally and spatially averaged temperature does not necessarily represent an equilibrium kinetic temperature.

The lifetime of the plasma of only a few nanoseconds is responsible for the reduction of thermal interactions with surrounding tissue, since, during such a short time period, heat cannot diffuse far into the tooth. Therefore, thermal cracks are avoided when ultra short laser pulses are used.

The difference in linewidth during the ablation of carious and healthy enamel is probably due to a slight difference in electron density, which might have a large effect on the shape of certain lines (21). The presented spectral differences demonstrate the possibility of distinguishing between carious and healthy enamel while ablating the tissue.

It is concluded that the preparation of enamel and dentine is possible using picosecond laser pulses, and no side-effects have yet been seen. However, the effectiveness of this laser type is still poor in comparison to conventional instruments. An in vivo application is not indicated yet because unwanted effects in living pulp cannot be excluded completely at this time.

ACKNOWLEDGEMENTS

The authors are grateful to Dr Ridder and Mr Himmelhaus of the PCI of the University of Heidelberg for their fruitful collaboration, and to Mrs Schagen of the Poliklinik für Zahnheilkunde of the University of Heidelberg for preparing the tooth samples.

REFERENCES

- 1 Boulnois JL. Photophysical processes in recent medical laser developments: a review. *Lasers Med Sci* 1986, 1:47–66
- 2 Stern RH, Sognnaes RF. Laser beam effect on dental hard tissues. *J Dent Res* 1964, 43:873

- 3 Goldman L, Hornby P, Mayer R, Goldman B. Impact of the laser on dental caries. *Nature* 1964, **203**:417
- 4 Stern RH, Vahl J, Sognaes RF. Lased enamel: ultrastructural observations of pulsed carbon dioxide laser effects. *J Dent Res* 1972, **51**:455
- 5 Frame JW. Carbon dioxide laser surgery for benign oral lesions. *Br Dent J* 1985, **158**:125
- 6 Zach K, Cohen G. Pulp response to externally applied heat. *Oral Surg* 1965, **19**:515-30
- 7 Frentzen M, Koort HJ, Kramer B. Thermische effekte bei der präparation von zahnhartgeweben mit verschiedenen lasersystemen. *Dtsch Zahnärztl Z* 1990, **45**:240-2
- 8 Keller U, Hibst R. Zur ablativen wirkung des Er:YAG Lasers auf schmelz und dentin. *Dtsch Zahnärztl Z* 1989, **44**:600-2
- 9 Hibst R, Keller U. Experimental studies of the application of the Er:YAG laser on dental hard substances I. *Lasers Surg Med* 1989, **9**:338-44
- 10 Keller U, Hibst R. Experimental studies of the application of the Er:YAG laser on dental hard substances II light microscopic and SEM investigations. *Lasers Surg Med* 1989, **9**:345-51
- 11 Liesenhoff T, Bende T, Lenz H, Seiler T. Grundlagen zur anwendung des excimer-lasers in der zahnheilkunde. *Dtsch Zahnärztl Z* 1990, **45**:14-6
- 12 Frentzen M, Koort HJ. Lasertechnik in der zahnheilkunde. *Dtsch Zahnärztl Z* 1991, **46**:443-54
- 13 Niemz MH, Eisenmann L, Pioch T. Vergleich von drei lasersystemen zur abtragung von zahnschmelz. *Schweiz Monatsschr Zahnmed* 1993, **103**:1252-6
- 14 Rechmann P, Hennig T, Kaufmann R. Laser in der Zahnhartsubstanzabtragung. *Zahnärztl Welt* 1992, **101**:150-60
- 15 Niemz MH. Investigation and spectral analysis of the plasma-induced ablation mechanism of dental hydroxyapatite. *Appl Phys B* 1994, **58**:273-81
- 16 Pioch T, Niemz M, Mindermann A, Staehle HJ. Schmelzablation durch laserimpulse im pikosekundenbereich. *Dtsch Zahnärztl Z* 1994, **49**:163-5
- 17 Haltenhoff U. *Mikrotomie in Biologie und Medizin*. Nussloch, Germany: Fr. Jung, 1979
- 18 Weast RC, Astle MJ. *CRC Handbook of Chemistry and Physics*. Boca Raton, Florida: CRC Press Inc., 1983
- 19 Huddlestone RH, Stanley LL (eds). *Plasma Diagnostic Techniques*. New York: Academic Press, 1965
- 20 Griem HR. *Spectral Line Broadening by Plasmas*. New York: Academic Press, 1974
- 21 Woltz LA, Hooper CF Jr. Calculation of spectral line profiles of multielectron emitters in plasmas. *Phys Rev A* 1988, **38**:4766-71

Key words: Picosecond laser; Nd-YAG laser; Nd-YLF laser; Dentistry; Caries removal